Analytic comparison of four robust algorithms for post-detection integration

N. Levanon

Indexing terms: Radar detection, Window integrator, Post-detection integration

Abstract: Four radar integration algorithms are compared with the basic moving window (video) integrator. The algorithms are robust in the sense of immunity against strong interfering spikes. Very strong spikes can appear if several radars operate in close proximity. The algorithms have been previously suggested for integration or are borrowed from CFAR thresholding methods. This paper provides an analytic performance analysis for a simple signal (Swerling II), noise and interference model. The comparison of the four algorithms, in the situation covered by this model, may be indicative of their relative performances in more realistic models, for which it is more difficult to obtain closed-form results.

1 Introduction

The sliding window integrator used extensively in radar detection is an efficient noncoherent integration method. However, integrating the signal amplitude directly makes it sensitive to interference spikes; a single infinitely strong spike will guarantee a false alarm. A classical remedy is the binary integrator (M-out-of-N) which exhibits inherent immunity to as many as $M-1$ spikes; as long as the number of strong spikes is smaller than M, the probability of a false alarm (P_{FA}) is smaller than one. The P_{FA} increases gradually from its nominal value towards unity as the number of strong spikes increases. The term 'robust' reflects this ability of the integration algorithm to maintain $P_{FA} \ll 1$ despite one or more infinitely strong interfering spikes. The price for this robustness is an added detection loss. Several other integration methods are considered, all with similar immunity against spikes. Of all the robust integration algorithms in this survey, the censored video integrator (CVI) suffers the smallest loss.

There is an analogy between integration of several pulse returns in fixed threshold detection and the process of estimating the mean level of the reference range-cells used in setting the adaptive threshold in CFAR detection. Immunity against interfering spikes in integration can be compared with immunity against interfering targets in the reference cells of a CFAR detector, and so most of the integration algorithms to be discussed here have twin algorithms in CFAR detection.

For a simple analysis, the algorithms are applied to the case of a Swerling II target in Gaussian noise. Recall that at the output of a square-law detector the normalised (with respect to the RMS noise) signal magnitude has a probability density function (PDF) and a distribution function given by

$$p(x) = D\exp(-Dx) \quad P(x) = 1-\exp(-Dx) \tag{1}$$

where $D = 1/(1+\overline{SNR})$. This PDF allows for simple analytic expressions of the detection and false alarm probabilities in the various integrators.

For the interference it is assumed that the spikes are infinitely strong. This asymptotic effect allows for a relatively simple analysis and yields the worst case increase of the P_{FA} due to interferences. It is also assumed that the probability of interference is very small and therefore the threshold will be set so that the nominal P_{FA} is reached when there are no interference spikes.

Paper 8414F (E5, E15), first received 12th November 1990 and in revised form 22nd May 1991

The author is with the Department of Electrical Engineering Systems, Tel-Aviv University, PO Box 39040, Tel-Aviv, 69978, Israel

2 Algorithms outline, threshold determination and performances (without interferences)

This section briefly describes the integration algorithms, and provides the relationship between P_{FA} and the threshold T for each algorithm. Assume that the threshold is set anticipating no interferences. Therefore, when considering the P_{FA}, the noise samples are assumed to be statistically independent and identically distributed (IID) according to eqn. 1 with $D = 1$. Similarly, when considering the probability of detection, the samples will be IID according to eqn. 1 with $D < 1$ (according to the SNR). It is sufficient to develop the equations for P_D and then set $D = 1$ to obtain the relationship between P_{FA} and the threshold.

2.1 Video integration

The video integrator (Fig. 1) sums all the N signal magnitude samples

$$y = \sum_{j=1}^{N} x_j \tag{2}$$

When x is IID according to eqn. 1, the PDF of y is well known:

$$p(y) = \frac{D^N}{(N-1)!}\, y^{N-1}\exp(-Dy) \tag{3}$$

Target detection is assumed when y exceeds a predetermined (normalised) threshold T. The probability of detection is therefore

$$P_D = 1 - P(T) \tag{4}$$

which yields

$$P_D = \exp(-TD)\sum_{r=0}^{N-1}\frac{(TD)^r}{r!} \tag{5}$$

The probability of a false alarm is obtained from eqn. 5 in the absence of signal:

$$P_{FA} = P_D|_{D=1} \tag{6}$$

For a given P_{FA} the normalised threshold T is obtained iteratively from eqn. 6. For $P_{FA} = 10^{-5}$, the normalised threshold as a function of the number of samples N is given in Table 1.

Of all the noncoherent integration methods, video integration is the most efficient, therefore the other methods are compared with it. The corresponding CFAR algorithm is the basic cell averaging CFAR. A major drawback of video integration is its sensitivity to interference. It is easy to see that one or more very strong spikes will result in the sum y exceeding the threshold,

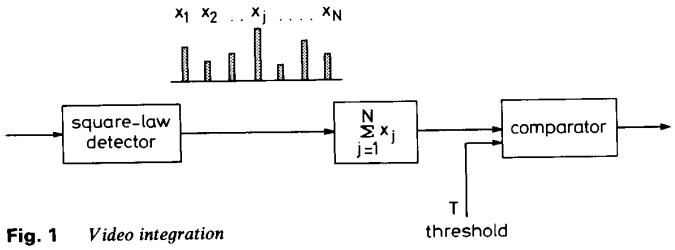

Fig. 1 *Video integration*

Table 1: Normalised threshold in video integration ($P_{FA} = 10^{-5}$)

N	10	9	8	7	6	5	4	3	2
T	29.522	27.842	26.123	24.358	22.538	20.648	18.666	16.554	14.237

even though the remaining samples are thermal noise samples. The next integration method overcomes this problem.

2.2 Binary integration (order statistics integration)

In binary integration [1, 2] each sample x_j ($j = 1, \ldots, N$) is compared to a threshold T (Fig. 2A). The analogue threshold is then followed by a binary one, which requires that at least M out of the total of N samples, have exceeded the analogue threshold.

From a mathematical standpoint, binary integration could also be called order statistics (OS) integration. The requirement for at least M-out-of-N threshold crossings is exactly the same as the requirement that the Kth ordered sample be larger than the threshold, where $K = N - M + 1$. From an engineering standpoint the implementation of OS integration (Fig. 2B) requires more processing. The analogue CFAR technique is Rohling's order statistics CFAR [3].

The analysis of binary integration can therefore follow OS analysis or cumulative probability analysis, and the end result will be the same. To follow the order statistics approach the distribution function of the Kth ordered sample, $P_K(x)$, is required:

$$P_K(x) = \sum_{r=K}^{N} \binom{N}{r} [P(x)]^r [1 - P(x)]^{N-r} \tag{7}$$

Substituting eqn. 1 in eqn. 7 and then in eqn. 4 gives

$$P_D = \exp(-TDN) \sum_{r=0}^{K-1} \binom{N}{r} [\exp(TD) - 1]^r \tag{8}$$

The threshold T is found iteratively from eqn. 8 after setting $D = 1$ and $P_D = P_{FA}$. The same threshold level applies to both methods of implementation, i.e. binary or order statistics. For $P_{FA} = 10^{-5}$ and $N = 10$, the normalised threshold as a function of K is given in Table 2.

Table 2: Normalised threshold in OS integration ($P_{FA} = 10^{-5}$, $N = 10$)

K	2	3	4	5	6	7	8	9
T	1.51	1.8785	2.2885	2.773	3.38	4.197	5.425	7.658

2.3 Censored video integration (CVI)

CVI is effectively a compromise between video integration and order statistics (binary) integration [4]. To censor the high ordered samples, it is first necessary to sort the samples according to magnitude. After sorting, the lowest K samples are integrated (Fig. 3), not, however, by simple addition. Whereas each of the lowest $K - 1$ ordered samples is given unit weight, the Kth ordered sample is given an additional weight. Epstein and Sobel [5] have shown that when the samples are

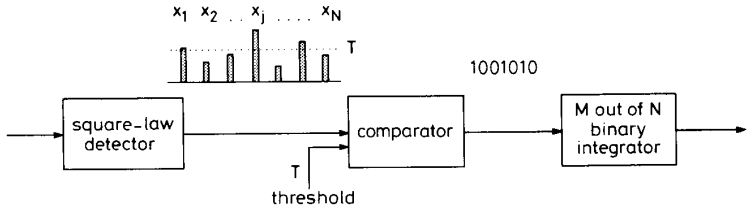

Fig. 2A *Binary integration*

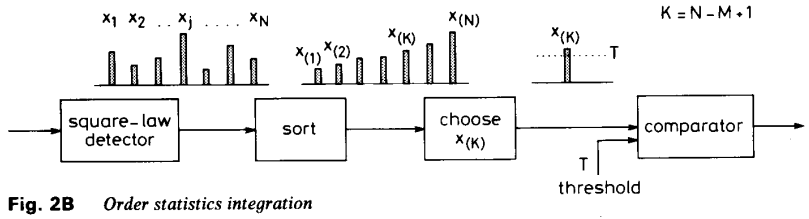

Fig. 2B *Order statistics integration*

exponentially distributed, the optimal weight of the Kth ordered sample is $N - K + 1$. Such a weight yields (after multiplication by N/K) an unbiased, minimum variance

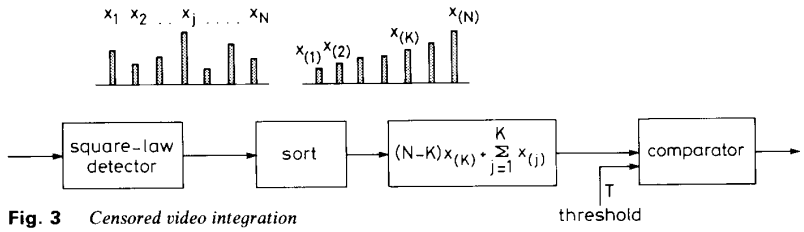

Fig. 3 *Censored video integration*

estimate of the original sum of the N samples. With this weighting, the integrator output is

$$y = (N - K)x_{(K)} + \sum_{j=1}^{K} x_{(j)} \tag{9}$$

In Reference 5 it was also found that the PDF of y is the same as that of the sum of only K samples of the exponentially distributed x_j, without sorting. Hence, all the results obtained for video integration (including Table 1), apply to censored video integration, after replacing N with K. Thus we get

$$P_D = \exp(-TD) \sum_{r=0}^{K-1} \frac{(TD)^r}{r!} \tag{10}$$

Again, the probability of a false alarm is obtained from eqn. 10 by setting $D = 1$. Table 1 applies here after replacing N with K.

Note that the corresponding CFAR technique is the censored mean level detector (CMLD) suggested by Ritcey [6].

2.4 Smallest-of integration

In this integration algorithm, the total number of pulses is divided in half, along the time axis. Each half is summed and the smallest of the two is used for comparison against a threshold (Fig. 4). The corresponding CFAR technique is the smallest-of (SO) CFAR proposed by Trunk [7]. The smallest-of approach protects against a burst of interference spikes, as long as they are all concentrated in a single half of the pulses.

The two sums are

$$y_L = \sum_{j=1}^{N/2} x_j \quad y_R = \sum_{j=1+N/2}^{N} x_j \tag{11}$$

and the threshold is compared with

$$y_{min} = \min(y_1, y_R) \tag{12}$$

In other words, both y_L and y_R have to exceed the threshold, yielding the square power of eqn. 5 with N replaced by $N/2$

$$P_D = \exp(-2DT)\left[\sum_{r=0}^{N/2-1} \frac{(DT)^r}{r!}\right]^2 \tag{13}$$

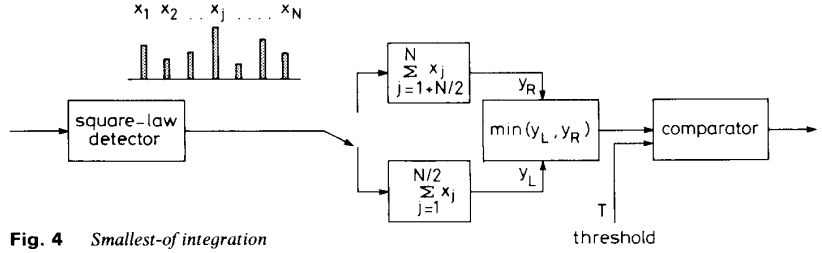

Fig. 4 *Smallest-of integration*

Again the probability of a false alarm is obtained from eqn. 13 by setting $D = 1$. Table 3 presents the relationship between T and N when $P_{FA} = 10^{-5}$.

Table 3: Normalised threshold in smallest-of integration ($P_{FA} = 10^{-5}$)

N	10	8	6	4	2
T	13.234	11.581	9.838	7.948	5.7565

2.5 Pairwise smallest-of integration

A modified version of the smallest-of integration was suggested by Linde [8]. His approach is to choose the smallest of each pair of consecutive samples and to sum these smaller samples (Fig. 5). In equation form, the algorithm compares the threshold with the random variable y, where

$$x_{[j]\min} = \min(x_j, x_{j-1}) \tag{14}$$

$$y = \sum_{j=1}^{N/2} x_{[2j]_{min}} \tag{15}$$

Since

$$p_{x_{[2j],\,min}}(x) = 2D \exp(-2Dx) \tag{16}$$

the expression for P_D is similar to eqn. 5:

$$P_D = \exp(-2TD) \sum_{r=0}^{N/2-1} \frac{(2TD)^r}{r!} \tag{17}$$

The relationship between T and N for $P_{FA} = 10^{-5}$ is given in Table 4.

Table 4: Normalised threshold in pairwise smallest-of integration ($P_{FA} = 10^{-5}$)

N	10	8	6	4	2
T	10.324	9.333	8.277	7.1183	5.7565

2.6 Added loss over video integration (without interference)

The penalty for the robustness is an added integration loss over the performances of the non-robust video-integrator. In the smallest-of and pairwise-smallest-of algorithms the number of samples used is always $N/2$, half the number of the original samples. The loss is therefore a function of the P_{FA}, N, and to a small extent also of P_D.

In the binary integrator and the CVI, we have the freedom to choose the number of samples used, namely

to choose K (or M where $M = N - K + 1$). Intuitively one would think that the added loss drops as K approaches N. As Fig. 6 shows, this is indeed true for the $P_D = 0.5$). Since $N = 10$ and $K = 8$, both the CVI and the binary integrator can tolerate up to two very strong interfering spikes, regardless of the position of the spikes.

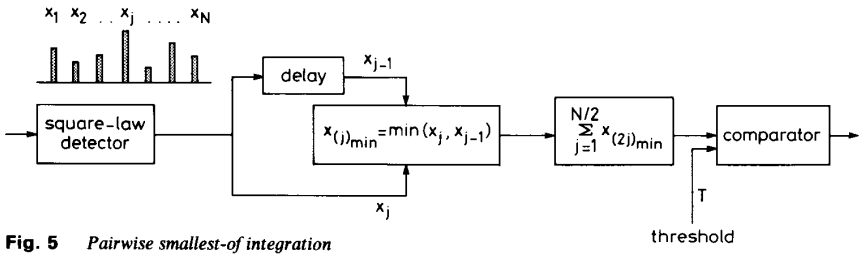

Fig. 5 *Pairwise smallest-of integration*

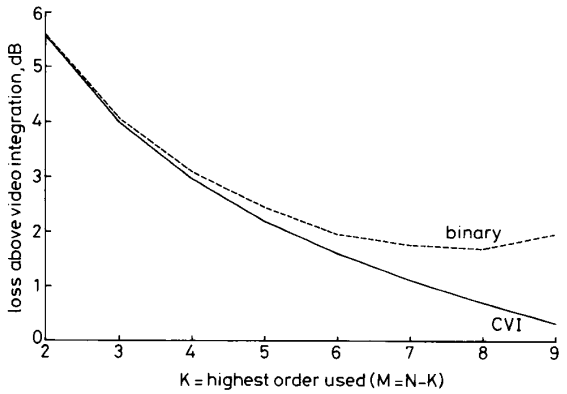

Fig. 6 *Additional integration loss as a function of the highest rank used, for censored video integration (CVI) and M-out-of-N binary integration*

$N = 10$, Swerling II, $P_{FA} = 10^{-5}$, $P_D = 0.5$

CVI but not for the binary integrator. In binary integration of $N = 10$ samples, the smallest additional loss was obtained with $K = 8$, $(M = 3)$. However, the loss dependence on K is rather flat for $K = 6$, 7, 8 and 9 (when $N = 10$). In comparing the four robust algorithms for the order statistics and the CVI we choose $K = 8$ when $N = 10$.

A comparison of the performances of the 3-out-of-10 binary integrator (BIN), a censored video integrator (CVI) with $K = 8$, a smallest-of integrator (SO), a pairwise smallest-of integrator (PSO), and the conventional video integrator (VID), is given in Fig. 7. Fig. 8 is an extension of Fig. 7 down to a very low SNR to demonstrate that the respective thresholds indeed lead to a $P_{FA} = 10^{-5}$ in all five cases.

Fig. 7 demonstrates that the CVI algorithm yields the smallest additional loss over video integration (0.7 dB at

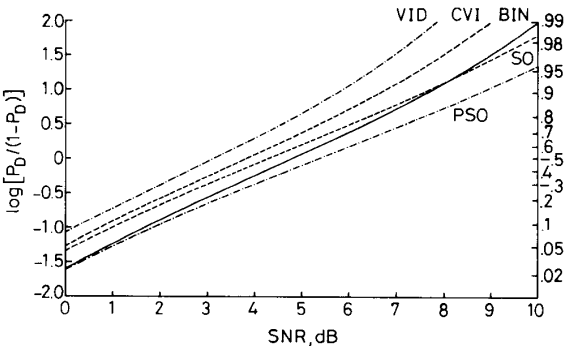

Fig. 7 *Detection performances of the five integration methods*

Swerling II, $N = 10$, $K = 8$ $(M = 3)$, $P_{FA} = 10^{-5}$

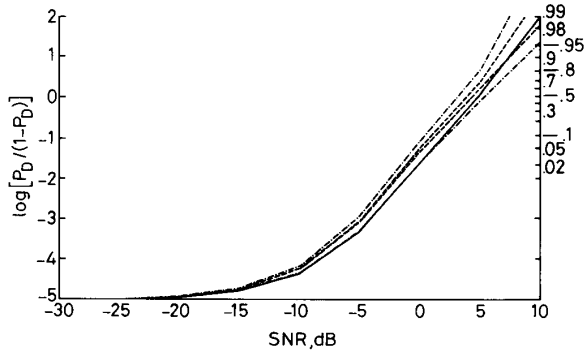

Fig. 8 *Extension of Fig. 7 to very low SNR, demonstrating* $P_{FA} = 10^{-5}$

Swerling II, $N = 10$, $K = 8$, $(M = 3)$, $P_{FA} = 10^{-5}$

The SO and PSO integrators can tolerate at least one spike, regardless of its position. The protection against additional spikes depends on their position relative to the first spike. With the spikes occurring at the most favorable locations, the SO and PSO algorithms can handle as many as five (out of ten) spikes. Detailed analysis of the performances in the presence of very strong interferences is given in the following Section.

3 Performances in the presence of infinitely strong interfering spikes

The major effect of strong interfering spikes is to increase the probability of a false alarm. This is discussed for the four algorithms. Assume that the threshold T was set to yield the nominal P_{FA} assuming no interferences, according to the relevant relationship between T and P_{FA}, as discussed in the preceding Section. We then find the increase in the P_{FA} due to the appearance of one or more infinitely strong spikes.

3.1 Binary (or order statistics) integration

The analysis of the effect of J infinitely strong spikes on the binary integrator (or order statistics integrator) is straightforward. Assume that the J strong spikes will occupy the top J ranks. To get a false alarm, the Kth ranked sample out of the remaining N-J pulses will have to cross the original threshold. The Kth ranked pulse out of a total of N-J pulses is statistically higher than the Kth ranking pulse out of N pulses. Hence the probability of a false alarm will increase.

The new probability of a false alarm will be obtained by simply replacing N in eqn. 8 by $N - J$, yielding

$$P_{FA}(J) = \exp\left[-T(N-J)\right] \sum_{r=0}^{K-1} \binom{N-J}{r} [\exp(T) - 1]^r \tag{18}$$

Recall that the threshold T is the original threshold obtained assuming no interfering spikes. In other words, T is found from the nominal P_{FA} and the above equation with $J = 0$.

3.2 Smallest-of integration

Smallest-of integration always protects against one strong spike. If additional spikes are present in the same half as the first spike they do not create any additional effect. However, an additional strong spike in the other half will cause a false alarm.

One spike (or up to $N/2$ spikes in the same half) will cause the algorithm to choose the sum of the other half as the smallest sum to be compared with the threshold. The PDF of this sum is simply the PDF of $N/2$ samples. Hence the false alarm will be given by the same equation as that of a simple video integrator operating on $N/2$ pulses. Thus, from eqns. 5 and 6,

$$P_{FA}(1) = \exp(-T) \sum_{r=0}^{N/2-1} \frac{T^r}{r!} \tag{19}$$

Recall again that the threshold in eqn. 19 is the original threshold obtained by setting $D = 1$ in eqn. 13.

If a second infinitely strong spike occurs, and its position is uniformly distributed among the remaining pulses, then the probability of a false alarm will obviously increase to

$$P_{FA}(2) = \frac{\frac{N}{2}}{N-1} + \frac{\frac{N}{2}-1}{N-1} P_{FA}(1) \approx \frac{N}{2(N-1)} \geqslant \frac{1}{2} \tag{20}$$

With the number of interfering spikes, J, increasing from 2 to N, the probability of a false alarm will increase from slightly above 0.5 to 1.

3.3 Pairwise smallest-of integration

When one sample is set very high by an interfering spike, its partner in the pair is automatically selected. The remaining pairs are not affected. Thus the new sum y will be effectively modified from the one given in eqn. 15. Without loss of generality, we assume that the interfering spike will coincide with the last pulse x_N, and get

$$y = x_{N-1} + \sum_{j=1}^{N/2-1} x_{[2j]min} \tag{21}$$

The PDF of each random variable in the sum is obtained from eqn. 16 by setting $D = 1$. Hence

$$P_{x[2j],min}(x) = 2 \exp(-2x) \tag{22}$$

The PDF of the individual sample is clearly the original PDF of a noise sample, namely

$$p(x) = \exp(-x) \tag{23}$$

Using the Laplace transform (with s representing the Laplace variable), we note that the PDF of y is

$$p(y) = \mathscr{L}^{-1}\left\{\left(\frac{2}{2+s}\right)^{N/2-1}\left(\frac{1}{1+s}\right)\right\} \tag{24}$$

which yields

$$p(y) = 2^{N/2-1} \exp(-y)\left[1 - \exp(-y) \sum_{r=0}^{N/2-2} \frac{y^r}{r!}\right] \tag{25}$$

Integrating $p(y)$ from the threshold T to infinity will yield the probability of a false alarm in the presence of one strong interfering spike:

$$P_{FA}(1) = 2^{N/2-1} \exp(-T)\left[1 - \exp(-T) \times \sum_{r=0}^{N/2-2} \sum_{k=0}^{r} \frac{T^k}{k!\, 2^{r-k+1}}\right] \tag{26}$$

If a second spike occurs and its position is uniformly distributed in any one of the remaining pulses, the probability that the second spike will coincide with the other member of the pair in which the first spike occurred is $1/(N-1)$. Such a coincidence will guarantee a false alarm, and its probability overshadows the probability of a false alarm when the spikes occur in two different pairs. Hence $P_{FA}(2)$ can be approximated by

$$P_{FA}(2) > \frac{1}{N-1} \tag{27}$$

With J increasing from 2 to N the probability of a false alarm will increase from slightly above $1/(N-1)$ to 1.

3.4 Censored video integration

As in order statistics integration here too the J strong spikes will occupy the top J ranks, reducing the effective number of pulses to N-J. However, the weighting law expressed in eqn. 9 is not aware that N was effectively reduced. Thus the PDF of the weighted sum is not equal any more to the PDF of K unsorted samples. Using eqn. 28 in Ritcey's work [6], the PDF of the sum will be given by an inverse Laplace transform,

$$p(y) = \mathscr{L}^{-1}\left\{\prod_{r=1}^{K}\left[1 + \left(\frac{N+1-r}{N-J+1-r}\right)s\right]^{-1}\right\} \tag{28}$$

An expression of $p(y)$ for any number of spikes J is too elaborate. After expanding the polynomial in eqn. 28 to a sum of simple fractions for $J = 1$, and inverting each fraction, we get

$$p(y) = \frac{(N-1)!}{(N-K-1)!} \times \sum_{r=N-K+1}^{N} \frac{r^{K-2}(-1)^{r+1}}{(N-r)![r-(N-K+1)]!} \times \exp\left(\frac{1-r}{r}y\right) \qquad J = 1 \tag{29}$$

Integrating $p(y)$ from T to infinity will yield the probability of a false alarm in the presence of one infinitely strong interfering spike:

$$P_{FA}(1) = \frac{(N-1)!}{(N-K-1)!} \times \sum_{r=N-K+1}^{N} \frac{r^{K-1}(-1)^{r+1}}{(r-1)(N-r)![r-(N-K+1)]!} \times \exp\left(\frac{1-r}{r}T\right) \tag{30}$$

For $J \geqslant 2$, eqn. 28 can be solved numerically and then integrated from T to infinity to obtain the P_{FA}. To complete Table 5, for the case of $N = 10$, $K = 8$, $T = 26.123$ and $J = 2$, P_{FA} yields 0.0179.

3.5 Summary of the interference effects

The increase of P_{FA} due to one or two infinitely strong spikes has been given analytically in the preceding Sec-

tions. To compare the performances, we present numerical results in Table 5 for the case of $N = 10$ pulses, $K = 8$, ($M = 3$) and a nominal $P_{FA} = 10^{-5}$. The normalised threshold, required to obtain the nominal P_{FA}, when there are no interfering spikes, is also listed in the Table. The theoretical results for the probabilities of a false alarm, with and without interfering spikes, were confirmed by Monte Carlo simulations.

Table 5 shows clearly that CVI is considerably less sensitive to spike interference than all the other algorithms. Combining this with its smaller detection loss leads to the conclusion that, from the point of view of performances, for the Swerling II case, CVI is superior to all the other integration algorithms discussed in this paper.

Table 5: P_{FA} in the presence of J infinitely strong interfering spikes out of $N = 10$ pulses

	T	$J = 0$	$J = 1$	$J = 2$
Binary $M = 3$ ($K = 8$)	5.425	1.00×10^{-5}	6.84×10^{-4}	0.0347
CVI $K = 8$	26.123	1.00×10^{-5}	3.66×10^{-4}	0.0179
Smallest-of	13.230	1.00×10^{-5}	3.17×10^{-3}	0.5570
Pairwise smallest-of	10.324	1.00×10^{-5}	5.23×10^{-4}	>0.111
Video	29.522	1.00×10^{-5}	1	1

4 References

1 HARRINGTON, J.V.: 'An analysis of the detection of repeated signals in noise by binary integration', *IRE Trans.*, 1955, **IT-1**, pp. 1–9

2 SCHWARTZ, M.: 'A coincidence procedure for signal detection', *IRE Trans.*, 1956, **IT-2**, pp. 135–139

3 ROHLING, H.: 'Radar CFAR thresholding in clutter and multiple target situations', *IEEE Trans.*, 1983, **AES-19**, pp. 608–621

4 LEVANON, N.: 'Censored video integration in radar detection'. Proceedings of IEEE International Radar Conference, Arlington, Virginia, May 1990, pp. 511–513.

5 EPSTEIN, B., and SOBEL, M.: 'Life testing', *J. Amer. Statistical Assoc.*, 1953, **48**, pp. 486–502

6 RITCEY, J.A.: 'Performance analysis of the censored mean-level detector', *IEEE Trans.*, 1986, **AES-22**, pp. 443–454

7 TRUNK, G.V.: 'Range resolution of targets using automatic detectors', *IEEE Trans.*, 1978, **AES-14**, pp. 750–755

8 LINDE, G.J.: 'Interference rejection and detection performance of the smallest of circuit'. NRL report 9243, Washington DC, November 1989